ELSEVIER

Chemical Geology 145 (1998) 395–411

CHEMICAL GEOLOGY
INCLUDING
ISOTOPE GEOSCIENCE

Thermal structure, thickness and composition of continental lithosphere

Roberta L. Rudnick *, William F. McDonough, Richard J. O'Connell

Department of Earth and Planetary Sciences, Harvard University, 20 Oxford St., Cambridge, MA 02138, USA

Received 10 January 1997; revised 27 August 1997; accepted 4 September 1997

Abstract

Global compilations of surface heat flow data from stable, Precambrian terrains show a statistically significant secular change from 41 ± 11 mW/m^2 in Archean to 55 ± 17 mW/m^2 in Proterozoic regions far removed from Archean cratons. Using the tectonothermal age of the continents coupled with average heat flow for different age provinces yields a mean continental surface heat flow between 47 and 49 mW/m^2 (depending on the average, non-orogenic heat flow assumed for Phanerozoic regions). Compositional models for bulk continental crust that produce this much or more heat flow (i.e., $K_2O > 2.3$–2.4 wt%) are not consistent with these observations. More rigorous constraints on crust composition cannot be had from heat flow data until the relative contributions to surface heat flow from crust and mantle are better determined and the non-orogenic component of heat flow in the areally extensive Phanerozoic regions (35% of the continents) is determined. We calculate conductive geotherms for 41 mW/m^2 surface heat flow to place limits on the heat production of Archean mantle roots and to evaluate the significance of the pressure–temperature (P–T) array for cratonic mantle xenoliths. Widely variable geotherms exist for this surface heat flow, depending on the values of crustal and lithospheric mantle heat production that are adopted. Using the average K content of cratonic peridotite xenoliths (0.15 wt% K_2O, assuming Th/U = 3.9 and K/U = 10,000 to give a heat production of 0.093 μW/m^3) and a range of reasonable crustal heat production values (i.e., ≥ 0.5 μW/m^3), we calculate geotherms that are so strongly curved they never intersect the mantle adiabat. Thus the average cratonic peridotite is not representative of the heat production of Archean mantle roots. Using our preferred estimate of heat production in the cratonic mantle (0.03 wt% K_2O, or 0.019 μW/m^3) we find that the only geotherms that pass through the xenolith P–T data array are those corresponding to crust having very low heat production (< 0.9 wt% K_2O). If the lithospheric mantle heat production is higher than our preferred values, the continental crust must have correspondingly lower heat production (i.e., bulk crustal K, Th and U contents lower than that of average Archean granulite facies terrains), which we consider unlikely. If the xenolith P–T data reflect equilibration to a conductive geotherm, then Archean lithosphere is relatively thin (150–200 km, based on intersection of the P–T array with the mantle adiabat) and the primary reason for the lower surface heat flow in Archean regions is decreased crustal heat production, rather than the insulating effects of thick lithospheric roots. On the other hand, if the xenolith P–T points result from frozen-in mineral equilibria or reflect perturbed geotherms associated with magmatism, then the Archean crust can have higher heat producing element concentrations, lithospheric thickness can range to greater depths and the low surface heat flow in Archean cratons may be due to the insulating effects of thick lithospheric roots. An uppermost limit for Archean

* Corresponding author. E-mail: rudnick@eps.harvard.edu

PII S0009-2541(97)00151-4

crustal heat production of 0.77 $\mu W/m^3$ is determined from the heat flow systematics.

Keywords: Thermal structure; Thickness of lithosphere; Composition of lithosphere; Continental lithosphere; Lithosphere

1. Introduction

Heat flowing from the surface of the earth can be divided into three components (Vitorello and Pollack, 1980): (1) heat from radiogenic decay of heat producing elements (HPE, mainly K, Th and U) in the lithosphere,[1] (2) heat conducted through the lithosphere from the underlying convective mantle and (3) 'orogenic' heat, convectively transported from magmas and fluids that enter the lithosphere from below during orogenic events. If these contributions to heat flow can be distinguished, it may be possible to place constraints on lithospheric composition (both crust and mantle) from heat flow data.

Nearly three decades ago it was discovered that surface heat flow correlates positively with heat production in particular heat flow provinces (Birch et al., 1968; Lachenbruch, 1968; Roy et al., 1968):

$$q_s = q_r + DA$$

where q_s is the surface heat flow, q_r is the reduced heat flow, D is the slope of the line (and broadly reflects the depth distribution of heat producing elements) and A is the heat production at the site where the heat flow is measured. The reduced heat flow was originally identified as the heat that originates from below the radiogenically-enriched upper crustal layer (Roy et al., 1968) and includes a mantle and deep crustal contribution to heat flow. Some subsequent workers have identified reduced heat flow with mantle heat flow in order to separate crust and mantle contributions to heat flow and place constraints on the heat producing element content of the continental crust.

However, recent work has shown that such an interpretation is likely to be in error, due to the combined effects of lateral heterogeneities in thermal conductivity and heat production within the crust (Jaupart, 1983; Furlong and Chapman, 1987; Pinet and Jaupart, 1987) and the possible effects of thick lithospheric mantle roots on heat flow from the convective mantle (Ballard and Pollack, 1987; Nyblade and Pollack, 1993). Therefore, constraints on crust composition from surface heat flow data are not as robust as was originally assumed by Taylor and McLennan (1985), who relied on the earlier heat flow models to derive their continental crust composition.

This paper consists of two parts. In the first part we review the constraints that heat flow data place on the composition of the continental crust. In the second part we investigate the bounds on heat producing elements abundances in the lithosphere of Archean cratons by comparison with surface heat flow and the temperature distribution in the lithosphere.

2. Composition of the continental crust

Table 1 lists models of the K, Th and U content for the bulk continental crust. These compositional estimates have been derived from observations of seismic velocities of the crust (Christensen and Mooney, 1995; Rudnick and Fountain, 1995; Wedepohl, 1995; Gao et al., 1998), chemical composition of granulite facies terrains (Weaver and Tarney, 1984; Shaw et al., 1986) and from heat flow observations combined with models of how the crust grows (Taylor and McLennan, 1985; McLennan and Taylor, 1996). There is over a factor of 2 difference in the K content between different estimates.

Constraining the K content of the continental crust is critical in mass balance calculations for the Earth. For example, if the crust has only 1.1–1.3% K_2O (Taylor and McLennan, 1985; McLennan and Taylor, 1996), it represents between 20–32% of the entire K budget of the silicate earth (SE) (Table 1).

[1] The term 'lithosphere' means different things to different people, depending upon the viewpoint of the user. In this paper we use 'lithosphere' to mean (a) the crust and that portion of the upper mantle mechanically coupled to the crust and (b) the crust and that part of the mantle through which heat is conductively transferred.

Table 1
K, Th and U concentrations, heat production and heat flow for various models of bulk continental crust and corresponding mantle heat flow

	K_2O (wt%)	Th (ppm)	U (ppm)	Silicate Earth K [a] (%)	Heat production [b] ($\mu W/m^3$)	Heat flow [c] (mW/m^2)	Mantle heat flow [d] (mW/m^2)
Bulk Crust Estimates							
Weaver and Tarney, 1984	2.1	5.7	1.3	37–52	0.92	38	9 to 11
Taylor and McLennan, 1985	1.1	3.5	0.91	20–27	0.58	24	23 to 25
Shaw et al., 1986	2.34	9.0	1.8	41–57	1.31	54	−5 to −7
Christensen and Mooney, 1995	2.1	(6.8)	(1.7)	37–52	1.12	45	2 to 4
Rudnick and Fountain, 1995	1.9	5.6	1.42	34–47	0.93	38	9 to 11
Wedepohl, 1995	2.4	8.5	1.7	42–59	1.25	51	−4 to −2
McLennan and Taylor, 1996	1.3	4.2	1.1	23–32	0.70	29	18 to 20
Gao et al., 1998	2.2	7.0	1.2	39–54	1.00	41	6 to 8
Archean Crust Estimates							
Weaver and Tarney, 1984 [e]	1.45	3.5	0.9		0.61	25	16
Taylor and McLennan, 1985	0.9	2.90	0.75		0.48	20	21
Rudnick and Fountain, 1995	1.2	3.0	0.7		0.50	20	21
McLennan and Taylor, 1996	1.2	3.8	1.0		0.64	26	15
Gao et al., 1998	2.4	6.4	1.0		0.93	38	3

Values in () are calculated assuming $K/U = 10^4$ and $Th/U = 3.9$.
[a] Assumes 180–250 ppm K in silicate earth, mass of crust is 0.00533 of BSE (see Galer et al., 1989, and references therein).
[b] Assumes density of 2800 kg/m^3.
[c] Assumes average crustal thickness of 41 km (Christensen and Mooney, 1995).
[d] Difference between mean surface heat flow (41 mW/m^2 for Archean and 47–49 mW/m^2 for bulk crust) and crustal heat flow.
[e] Assumes Archean upper crust composition of Taylor and McLennan (1985).

Thus all of the K in the continental crust can be derived from the upper mantle alone (i.e., that portion above the 670 km seismic discontinuity), which constitutes ~27% by mass of the SE (Galer et al. (1989) and references therein). In all other estimates, the crust contains more K than could have existed in a primitive upper mantle alone, requiring significant mass input from the lower mantle (Table 1).

The crustal values of K, Th and U adopted by Taylor and McLennan (1985) and McLennan and Taylor (1996) stand out as being lower than the other models. These authors used surface heat flow to constrain the bulk continental crust composition. Below we evaluate the heat flow data to determine what limits may be placed on crustal K content from surface heat flow.

2.1. Observations and broad constraints from heat flow

In the absence of knowledge concerning the partitioning of heat flow from crust versus mantle, only very broad constraints can be placed on crustal composition. To do this, surface heat flow data from stable continental regions that have remained isolated from orogenic activity since the end of the Precambrian are utilized. Using these data from a global compilation, Nyblade and Pollack (1993) made the following observations:

(1) Proterozoic crust within 100 to 400 km of Archean cratons has low heat flow, similar to that within the nearby craton. The width of these low heat flow pericratonic regions seems to correlate with location. In North America they are the largest, from 300–400 km wide, those in Europe are intermediate, whereas those in Africa are typically 100–200 km wide.

(2) The mean surface heat flow in Archean cratons is 41 ± 12 mW/m^2 (188 observations, uncertainty is one standard deviation of mean) and for stable Proterozoic crust beyond 100–400 km from Archean craton boundaries is 55 ± 17 mW/m^2 (342 observations) (Table 2).

The lower heat flow in Archean cratons may be the result of intrinsically lower heat production in

Table 2
Estimates of non-orogenic surface heat flow for the continental crust

Tectonothermal Age	Mean heat flow [a], (mW/m^2)	Standard deviation [a]	*n*	Areal extent [b] (%)
Archean	41	11	188	20
Early Proterozoic	46	15	113	12
Late Proterozoic	49	16	562	33
Proterozoic far removed from Archean	55	17	342	
Phanerozoic	49–55 [c]			35
Total continents	47–49			

[a] From Nyblade and Pollack (1993), table 2.
[b] From Sclater et al. (1980), fig. B2.
[c] Estimated to range between the average late Proterozoic value and the average Proterozoic crust, far removed from Archean cratons.

their crust (Morgan, 1984; Nyblade and Pollack, 1993) or may result from refraction of heat flow from Archean cratons due to the presence of thick mantle roots (Ballard and Pollack, 1987; Nyblade and Pollack, 1993). These explanations are not mutually exclusive and both may play a role in explaining the observed heat flow patterns. The Proterozoic pericratonic regions of low heat flow are also compatible with either explanation: they may be regions having only a thin, tectonically transposed slice of Proterozoic crust overlying Archean crust and mantle roots, or they may be largely re-worked Archean crust (Nyblade and Pollack, 1993).

The global compilation described above provides mean surface heat flow values for stable crustal regions, free of orogenic heat, that may be used to determine the non-orogenic, continental surface heat flow for crust of various tectonothermal ages (Table 2). We used these values, weighted according to the tectonothermal age distribution of the crust (according to the model of Sclater et al., 1980) to estimate the average, non-orogenic, surface heat flow from the continents. For Phanerozoic regions, which often show the effects of advective heat transfer (Vitorello and Pollack, 1980), we assume that the non-orogenic heat flow component 1) is equal to the average observed for late Proterozoic crust (i.e., 49 mW/m^2) or 2) is equal to the average observed for Proterozoic crust far removed from the influence of Archean cratons (i.e., 55 mW/m^2, Fig. 4b of Nyblade and Pollack, 1993). In this manner the average, non-orogenic heat flow from the continents is estimated to lie between 47 and 49 mW/m^2. In order for a crust composition model to be viable, it must produce less heat than this.

2.1.1. Crustal models

The heat generated by model crust compositions can be calculated from the K, Th and U concentrations, given density and crustal thickness (Fig. 1). Throughout this paper we assume a mean crustal density of 2800 kg/m^3 and an average crustal thickness of 41 km (Christensen and Mooney, 1995). Table 1 shows heat production for the various model compositions of continental crust and corresponding heat flow for a 41 km thick crust.

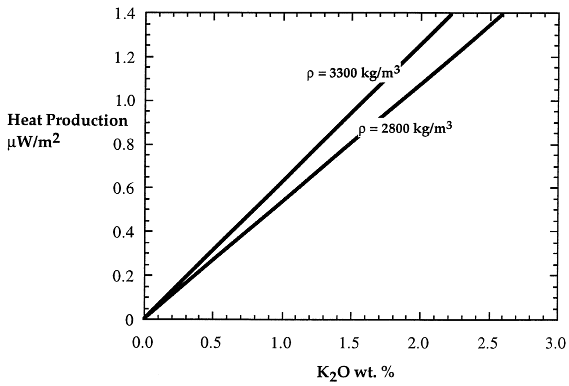

Fig. 1. K_2O content (in weight %) versus heat production for two densities: 2800 kg/m^3, representative of crustal rocks and 3300 kg/m^3, representative of mantle peridotite, assuming $K/U = 10,000$ and $Th/U = 3.9$. Compositions that deviate from these assumed proportions of K, Th and U will not plot on these lines.

2.1.1.1. Archean crust. Many of these models do not distinguish Archean from post-Archean crust. The exceptions: Taylor and McLennan (1985), McLennan and Taylor (1996) and Rudnick and Fountain (1995), produce 20, 26 and 21 mW/m^2 heat flow, respectively, for a 41 km thick Archean crust. The Weaver and Tarney (1984) crustal model is based on analyses of amphibolite and granulite facies rocks from the Archean Lewisian complex, Scotland. Although these authors adopt Taylor and McLennan (1981) upper crust composition in their model, an estimate of Archean crustal composition can be had by substituting the Taylor and McLennan (1985) Archean upper crustal composition into their model. Doing this gives an Archean crustal heat flow of 25 mW/m^2, illustrating that the high heat production of the Weaver and Tarney model is mainly a function of their assumptions about the proportion and composition of the upper continental crust. These values for crustal heat flow are 50–93% of the observed surface heat flow in Archean regions and thus lie well within the upper bounds of the heat flow data.

Recently, Gao et al. (1998) estimated the composition of crust in the Archean North China craton. They report a relatively high heat production of 0.93 $\mu W/m^3$, which corresponds to a surface heat flow of 33.5 mW/m^2 for the thin (36 km) crust in this region. North China also has high heat flow (60 mW/m^2) compared to stable Archean regions, due to Cenozoic rifting. If the heat production values estimated by Gao et al. are assigned to a 41 km thick crust, it produces a surface heat flow of 38 mW/m^2. This value is too high to be representative of average Archean crust, where the surface heat flow is 41 mW/m^2. This discrepancy may be explained if the presently thin crust resulted from the loss of a mafic lower crust, which had low heat production (Gao et al., 1998). However, if true, the original crust would still have contributed ~80% of the present average surface heat flow in stable Archean regions. This value is higher than any current estimate of the crustal contribution heat flow in stable Archean regions (Pinet and Jaupart, 1987; Pinet et al., 1991) and would also result in unrealistically cool and extraordinarily thick mantle lithosphere (see Fig. 6a, Fig. 7 and discussion below). Alternatively, the values of Gao et al. may reflect an unusually HPE-rich crust in northern China (i.e., the surface heat flow was never as low as 41 mW/m^2, even before the Cenozoic rifting).

2.1.1.2. Bulk crust. The two most radiogenic models for the bulk continental crust, those of Shaw et al. (1986) and Wedepohl (1995), produce heat flow approaching the value for stabilized post-Archean crust (54 and 51 mW/m^2, respectively, compared to 55 mW/m^2) and are higher than the mean crustal heat flow calculated above (47 to 49 mW/m^2). These models produce more heat than the entire mean surface heat flow from the continents. If the values we used for mean surface heat flow are correct, these crust compositional models can be ruled out as being too enriched in HPE.

The remaining models of bulk crust have heat productions lower than the mean surface heat flow and therefore are compatible with heat flow constraints. The more radiogenic crustal models (Weaver and Tarney, 1984; Christensen and Mooney, 1995; Rudnick and Fountain, 1995; Gao et al., 1998) allow for less mantle heat flux (between 2 and 11 mW/m^2) than the relatively depleted model of Taylor and McLennan (1985) and McLennan and Taylor (1996) (18 to 29 mW/m^2).

2.2. Unraveling crust and mantle contributions to heat flow

Although the heat flow data themselves do not allow the relative contributions of crust and mantle to be deciphered, incorporation of geochemical data for crustal cross sections and seismic velocities of the lower crust can be used towards this end. However, there are two drawbacks to this method:

1. none of these cross sections provides a complete section through the crust —invariably the lowermost crust is missing and sometimes the uppermost crust, and
2. as with any study of deep crustal rock types (e.g., xenoliths, granulite facies terrains) it is unknown how representative the cross sections are of the crust in general.

To compensate for the first problem, some workers utilize seismic velocity data for the regions of interest to infer rock types present in the lowermost crust and couple this information with HPE contents of lower crustal xenoliths and high pressure granulite terrains (Rudnick and Fountain, 1995; Ketcham, 1996). In the absence of seismic data, upper and lower bounds can be placed on the heat production of the missing lowermost crust based on comparisons with rocks in granulite terrains and xenolith suites (e.g., Rudnick and Fountain, 1995).

Table 3 summarizes the findings of crustal cross-section studies. The heat flow values assume a 41 km thick crust and mean surface heat flow of 41 and 55 mW/m^2 for Archean and post-Archean regions, respectively. A similar compilation by Rudnick and Fountain (1995, Table 3) used the regional crustal thickness and heat flow values (where possible) to determine crustal heat production and heat flow for the individual sections. Differences between our numbers and this earlier study reflect deviations of local areas from the assumed heat flow and crustal thickness values adopted here.

The following assumptions were made regarding the missing sections of crust: for the Archean Vredefort, Kapuskasing and Pikwitonei sections, between 15 and 21 km of the lowermost crust is unexposed. We assume average heat production in this lowermost crust ranging from 0.06 $\mu W/m^3$ (median mafic granulite from Rudnick and Fountain, 1995), to 0.4 $\mu W/m^3$ (mean granulite facies terrain for Archean crust, Pinet and Jaupart, 1987) to obtain the values shown in Table 3. In the Lewisian section it is the upper crust that is not present. Weaver and Tarney (1984) assumed that the upper one third of the crust has a composition of Taylor and McLennan (1981) average upper continental crust. As discussed above, this is the main reason for the radiogenic value of their bulk crust. For the purposes of producing a representative Archean crustal section, we use Taylor and McLennan (1985) average Archean upper crust to come up with the Lewisian crustal heat flow values listed in Table 3.

Sections through Proterozoic aged crust are available from Scandinavia and North America. In Southern Scandinavia Pinet and Jaupart (1987) estimate an average crustal contribution to heat flow of 31 mW/m^2 using a combination of heat flow data, gravity data and measured heat production for a variety of mid- to deep-crustal rock types. In southern Norway, where the thickest crust occurs, Pinet and Jaupart (1987) estimate that the crust consists of 7 km of amphibolite facies rocks and granites overlying 28 km of granulite facies rocks. Scaling these proportions to a 41 km thick crust yields a crustal contribution to heat flow of 35 mW/m^2. In other areas (e.g., Egersund area) the crust is thinner (28 km), high grade rocks crop out at the surface, crustal radioactivity is consequently lower (average 0.4 $\mu W/m^3$), and the surface heat flow is only 21 mW/m^2. Assuming that the missing 13 km of crust had a composition of average upper crust (Taylor and McLennan, 1985) yields a crustal contribution to heat flow of 34 mW/m^2. Thus, the southern Scandinavia data suggest a range in crustal heat flow of 34–35 mW/m^2.

Ketcham (1996) describes the vertical distribution of heat producing elements for two reconstructed sections through Proterozoic crust in metamorphic

Table 3
Crustal and mantle contributions to heat flow as determined from crustal cross sections

Locality	Heat flow contributions (mW/m^2)		Reference
	Crust[a]	Mantle[b]	
Archean		*Mean Surface Heat Flow = 41 mW/m^2*	
Vredefort, South Africa	29–36	5–12	Nicolayson et al. (1981)
Lewisian, Scotland	25–30	11–16	Weaver and Tarney (1984)
Kapuskasing, Ontario	23–28	13–18	Ashwal et al. (1987)
Pikwitonei, Manitoba	20–23	18–21	Fountain et al. (1987)
Proterozoic		*Mean Surface Heat Flow = 55 mW/m^2*	
S. Norway	34–35	20–21	Pinet and Jaupart (1987)
Catalina Core Complex, AZ	$>$ 26–34	$<$ 21–29	Ketcham (1996)
Harquahala Core Complex, AZ	$>$ 32–44	$<$ 11–23	Ketcham (1996)

[a] 41 km thick. See text for description of assumptions made regarding the unexposed portions of the crust.
[b] Calculated as difference between surface heat flow and crustal heat flow.

core complexes of the southwestern U.S. The reconstructed sections reach depths of only 13 to 14 km, so the heat production of the lower crust is estimated from studies of lower crustal xenoliths and seismic refraction data. Ketcham (1996) calculates a total crustal contribution to heat flow between 32 to 44 mW/m^2 for a 30 km thick crust in the Harquahala complex and 26–34 mW/m^2 for a 32 km crust in the Catalina complex. These sections occur in extended crust, which is thinner than average continental crust by 11 and 9 km, respectively. The heat flow from average thickness continental crust will be higher than these estimates, depending on the nature of the material removed by thinning. These estimates for Proterozoic crust are therefore illustrated in Fig. 2 with arrows to indicate they represent minimum values of the crustal contribution to heat flow.

Fig. 2 compares the crustal cross-section observations with different models of crust composition. The measured cross sections show crustal contributions to heat flow ranging from 20 to > 44 mW/m^2, with Proterozoic cross sections overlapping the highest values of Archean sections. Although limited, these data lend support to a difference in crustal radioactivity between Archean and Proterozoic crust. The Wedepohl (1995) and Shaw et al. (1986) crustal models generate more heat than any of the crustal cross sections, while the remaining models fall within the range of values observed in crustal cross sections.

In summary, the crustal cross-section data allow comparisons to be made between crustal compositional models and crustal heat production from specific areas. The most radiogenic crustal models (those of Shaw et al., 1986 and Wedepohl, 1995) lie beyond the crustal contribution to heat flow inferred for any crustal sections measured to date. Thus, in agreement with a recent analysis of the heat flow data (McLennan and Taylor, 1996), we believe the models of Shaw et al. (1986) and Wedepohl (1995) can be ruled out as being too enriched in HPE. However, in contrast to McLennan and Taylor (1996), we believe the heat flow data cannot be used to place any tighter constraints on crustal composition until a better understanding of the relative contributions from crust and mantle is achieved. Towards this end there is a clear need for more crustal cross-section data.

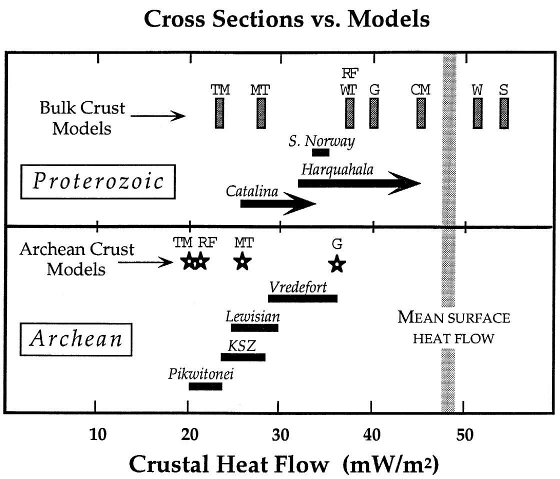

Fig. 2. Comparison of crustally generated heat flow estimated from crustal cross sections (Table 3) and model crust compositions (Table 1). Archean crustal models shown as stars in lower panel. Bulk crustal models shown as vertical bars in upper panel. The gray vertical band marks the range of mean surface heat flow for stable continental crust, as estimated in the text and Table 2. *TM* = Taylor and McLennan (1985), *MT* = McLennan and Taylor (1996), *RF* = Rudnick and Fountain (1995), *WT* = Weaver and Tarney (1984), *G* = Gao et al. (1998), *CM* = Christensen and Mooney (1995), *W* = Wedepohl (1995), *S* = Shaw et al. (1986).

3. Composition and thermal structure of cratonic lithospheric mantle

The lithospheric mantle represents another potential source of heat within the continents and, although the concentrations of HPE are clearly much lower in mantle than in crustal rocks, the great thickness of lithospheric mantle that may exist beneath some crustal regions (e.g., cratons) makes mantle lithosphere a potentially important contributor to surface heat flow (Jordan, 1988).

Unfortunately, the lithospheric mantle is much less accessible than the continental crust so its heat production is even less well constrained. There are no continuous tectonic cross sections through lithospheric mantle and our understanding of its heat production rests solely on the few samples available for study: tectonic slices of lithospheric mantle in orogenic regions (massif peridotites) and mantle xenoliths. On the bright side, however, the lithospheric mantle shows less lithologic diversity than the continental crust and the dominant rock type, peridotite, has relatively limited variation in major element compositions (42–48 wt% SiO_2, 35–50 wt% MgO, and 7 $\pm$ 2 wt% FeO). In addition to peridotite, the continental lithospheric mantle contains small amounts of other lithologies including eclogites, pyroxenites, and megacrystalline assemblages (e.g., MARID (mica–amphibole–rutile–ilmenite–diopside) Dawson and Smith, 1977). Statistical studies of xenolith and xenocryst populations (Sobolev, 1977; Schulze, 1995) and mapping of massif bodies suggest that these other lithologies are subordinate to peridotite in the continental lithospheric mantle. In addition to uncertainties in their volumetric proportions, these other lithologies display a broad compositional range (particularly with respect to their HPE contents), making it difficult to establish a meaningful estimate of their average composition. Here we restrict our analysis to peridotites with the proviso that small amounts of highly enriched material are present locally.

To place constraints on the amount of heat production in the continental lithospheric mantle we calculate a family of conductive geotherms (following Chapman, 1986), making various assumptions regarding the amount and distribution of heat producing elements in the lithosphere. We limit our discussion here to stable Archean cratons, where the heat flow is relatively low and uniform (41 $\pm$ 11 mW/m^2), consistent with the assumption of conductive heat transport, and where thermobarometry of garnet-bearing peridotites has defined possible paleogeotherms present at the time of eruption of the host kimberlites (i.e., Cretaceous in South Africa and Paleozoic in Siberia). We compare our results to the observed heat production of various mantle samples in order to place an upper limit on the concentration of heat producing elements in cratonic mantle roots.

3.1. Geotherm calculations

There are several broad constraints on heat source abundance and distribution in the lithosphere that can be had from consideration of heat flow and lithospheric thermal structure. The first is that the heat production in the crust and lithospheric mantle cannot exceed the measured heat flow at the surface. This assumes that a conductive thermal steady state exists, and that transients and advective heat transport do not contribute substantially to the heat flow. This assumption is supported by the age and stability of the cratons, although the relatively recent emplacement of kimberlites and, in some cases, flood basalts, indicates that there may be some transients; the comparisons we make with kimberlitic xenolith thermobarometry data later bear on this.

A second constraint is that the geotherm that results from a given model is reasonable. The conductive geotherm is determined solely by the heat flux at the surface and the distribution of heat sources; there is no a priori requirement that it meet an adiabatic geotherm at depth. However, for a model to be reasonable, a conductive geotherm in the lithosphere must intersect an adiabatic geotherm at the base of the lithosphere. We use this condition to assess the reasonableness of various models of heat source distribution in the crust and lithospheric mantle.

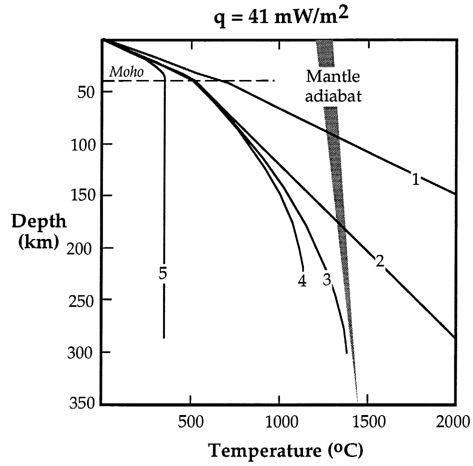

Fig. 3. Model geotherms illustrating the effects of various lithospheric heat source distributions for a surface heat flow of 41 mW/m^2. Also shown is a range of mantle adiabats with which a reasonable geotherm should merge at the base of the lithosphere (see text). Curve 1 has no lithospheric heat sources, and intersects the adiabat at 85 km. Curve 5 produces all the surface heat flow from crustal heat sources; the temperature is constant with depth (and low) beneath the crust, and results in an unreasonable geotherm. For curves 2, 3, 4 half of the surface heat flow is produced in the crust. Curves 2 and 3 produce reasonable geotherms that meet the adiabat, but curve 4 has mantle heat sources that are too high, and it never reaches the adiabat. Other parameters as in Table 3.

These considerations are illustrated in Fig. 3 for a surface heat flow of 41 mW/m^2. A mantle adiabat with a surface temperature of 1200 to 1300°C is shown. Curve 1 shows the temperature distribution for the limiting case with no heat sources in the crust or mantle. This is a straight line that intersects the adiabat at ~85 km, which would then represent the base of the lithosphere. This model produces a Moho temperature of 700°C. Curve 5 shows the result for the other limiting case, where the heat sources in the crust are sufficient to produce all of the surface heat flow. In this case the Moho temperature is half of the previous case's value, and the temperature is constant in the lithospheric mantle (which has no heat sources). The lithospheric mantle heat flow is zero. Obviously, this geotherm cannot merge with an adiabat at any depth and thus is not a reasonable model.

The other curves represent half of the surface heat flow coming from crustal heat sources. Curve 2 has no heat sources in the lithospheric mantle; the base of the lithosphere is at 180 km, and the heat flow is constant throughout the mantle root. This produces a reasonable model. Curve 3 has heat sources in the mantle (0.05 μW/m^3) and merges with the adiabat near 300 km, where the heat flux from the convecting mantle is 0.7 mW/m^2. This then produces a reasonable model with a 300 km lithosphere. Curve 4 (heat sources 0.07 μW/m^3) on the other hand produces a geotherm that bends over at 250 km where it is 250°C colder than the adiabat. This distribution of heat sources does not produce a reasonable geotherm.

There are a number of parameters that must be considered when calculating conductive geotherms. Table 4 lists these along with the assumptions we make regarding their values. Our approach is to hold most parameters constant, varying only crustal and mantle heat production to see how this affects lithospheric thickness, as defined by the intersection of the conductive geotherm with the mantle adiabat. We also compare our results with the P–T data arrays recorded by cratonic mantle xenoliths.

We assume a range of mantle adiabats corresponding to potential temperatures between 1200 to 1300°C. These are consistent with experimental evidence for the temperature of the 410 km phase transition (Akaogi et al., 1989; Ito and Takahashi, 1989) and plausible adiabatic gradients of 0.3 to 0.5°C/km (Fei, 1995; Navrotsky, 1995). The continental crust is assumed to be 41 km thick and consists of three layers. The majority of heat production occurs in the upper $\frac{1}{3}$ of the crust, the middle crust has lower, but still significant heat production and only very low heat production occurs in the

Table 4
Parameters used in cratonic geotherm calculations

Parameters held constant	
Crustal density	2800 kg/m^3
Lithospheric mantle density	3300 kg/m^3
Crustal thickness	41 km [a]
Thermal conductivity —crust	2.6–2.7 W/m°C, varying with depth [b]
Thermal conductivity —mantle	T-dependent model [b]
HPE distribution in crust	3 layers of equal thickness [d]: 60% Upper crust, 34% Middle crust, 6% Lower crust
HPE distribution in mantle	Constant with depth
Mantle potential temperature	1200–1300°C
Surface heat flow	41 mW/m^2
Bounds for changing parameter	
Crustal heat production	0.4–0.7 μW/m^3
Lithosphere thickness	200–400 km
Lithospheric mantle heat production	0.02–0.10 μW/m^3

[a] Christensen and Mooney, 1995.
[b] Chapman, 1986.
[c] Schatz and Simmons, 1972.
[d] Rudnick and Fountain, 1995.

lower crust (Table 3, Rudnick and Fountain, 1995). As demonstrated previously, changing the crustal distribution of HPE has only minor effects on the Moho temperature (Davies and Strebeck, 1982; Chapman, 1986) and does not affect the shape of the mantle geotherm.

The calculated geotherms are particularly sensitive to the absolute heat production in the continental crust. From the discussion above, we can place only broad constraints on this parameter for Archean regions. The minimum heat production of Archean crust is greater than 0.4 $\mu W/m^3$ —the average heat production of Archean granulite facies terrains (Pinet and Jaupart, 1987), which are depleted in HPE. Clearly the crust is not composed of granulites from top to bottom. The maximum heat production for Archean crust is taken as 0.7 $\mu W/m^3$. This corresponds to a crustal heat flow of 29 mW/m^2, or 12 mW/m^2 heat flux across the Moho —equivalent to the minimum mantle heat flux estimated for Archean regions (Pinet and Jaupart, 1987; Pinet et al., 1991).

3.2. Heat production in peridotites and constraints on Archean lithospheric mantle composition

Given these bounds we explore the range of possible HPE content of the lithospheric mantle. Lithospheric peridotites are available from three sources:

1. xenoliths carried in lavas (kimberlites and alkaline extrusives) that erupt through Archean cratons. We call these 'cratonic' peridotites following earlier usage (e.g., Boyd, 1989),
2. xenoliths carried in alkali basalts that erupted in Proterozoic and younger continental regions ('off-craton' peridotites), and
3. massif peridotites, which are tectonic fragments of upper mantle interleaved with crustal rocks in Phanerozoic fold belts.

Chemical analyses of cratonic peridotites are available mainly for South African and, to a lesser extent, Siberian samples. However, we also include in this peridotite category two localities where xeno-

Table 5
Mean and median values of peridotites from different settings

	Off-craton				On-craton					
	Massifs		Sp perid. xenoliths		All		Kimberlite hosted		Non-kimberlite hosted	
	Mean	Median	Mean	Median	Mean	Median	Mean	Median	Mean	Median
SiO_2	45.00	45.05	44.02	44.16	45.20	45.18	45.45	45.44	43.70	43.80
TiO_2	0.15	0.13	0.11	0.09	0.11	0.08	0.11	0.08	0.11	0.08
Al_2O_3	2.76	2.89	2.33	2.25	1.33	1.76	1.41	1.21	0.87	0.56
Cr_2O_3	0.38	0.37	0.39	0.39	0.41	0.37	0.42	0.37	0.38	0.38
FeO_{total}	8.25	8.05	8.38	8.14	7.43	7.44	7.32	7.35	8.09	7.71
MnO	0.13	0.13	0.14	0.14	0.15	0.12	0.15	0.11	0.12	0.12
MgO	40.62	40.25	41.35	41.05	44.42	44.70	44.18	44.48	45.85	46.30
NiO	0.26	0.26	0.27	0.27	0.32	0.28	0.32	0.28	0.36	0.35
CaO	2.44	2.51	2.18	2.27	1.10	0.83	1.09	0.83	1.11	0.75
Na_2O	0.22	0.20	0.24	0.21	0.11	0.07	0.11	0.08	0.09	0.07
K_2O	0.029	0.010	0.052	0.020	0.148	0.070	0.166	0.080	0.045	0.030
P_2O_5	0.03	0.02	0.05	0.03	0.02	0.01	0.02	0.01	0.02	0.01
Mg#	89.8	89.9	89.8	90.0	91.4	91.5	91.5	91.6	90.9	91.4
K (ppm)	242	86	430	166	1228	581	1378	664	370	249
n		130		366		486		416		70
Th *	0.095	0.034	0.168	0.065	0.479	0.227	0.537	0.259	0.144	0.097
U *	0.024	0.009	0.043	0.017	0.123	0.058	0.138	0.066	0.037	0.025
Heat prod.[a] $\mu W/m^3$	0.018	0.006	0.033	0.013	0.093	0.044	0.104	0.050	0.028	0.019

* Calculated from K/U = 10,000 and Th/U = 3.9
[a] Assumes density of 3300 kg/m^3.

liths are carried in alkali basalts or lamprophyres that erupt through Proterozoic crust: Tanzania and the Colorado plateau. The garnet peridotites in both these localities have mineralogical, textural and chemical properties similar to peridotites from the Kaapvaal and Siberian cratons (Rhodes and Dawson, 1975; Ehrenberg, 1982; Rudnick et al., 1994). Indeed, preliminary Os isotope data for the Tanzanian peridotites shows that some, perhaps all, experienced Re (hence melt) depletion in the Archean (Chesley and Rudnick, 1996). These localities will prove to be important in our endeavor to establish the heat production of cratonic mantle lithosphere, as they are generally free from the extensive alteration (including development of secondary HPE-bearing phases) that is ubiquitous in kimberlite-hosted peridotite xenoliths (see below).

Peridotites in all groups display a range of major element compositions from fertile lherzolite (similar to the primitive mantle's composition) to strongly depleted harzburgite and dunite. The range in bulk composition is generally interpreted to reflect the average degree of melt depletion, with cratonic peridotites being the most refractory (Boyd, 1989; Hawkesworth et al., 1990; McDonough, 1990), and thus showing the greatest loss of melt (Table 5). Paradoxically, the most refractory peridotites show the greatest enrichments of incompatible trace elements (see McDonough and Frey, 1989, and references therein). This observation is generally attributed to secondary enrichment processes (i.e., metasomatism) that have not, for the most part, affected regions of the mantle sampled by massif peridotites.

Table 5 shows the average and median compositions of the three groups of peridotites. Cratonic peridotites have the highest concentrations of HPE, followed by off-craton spinel peridotites and finally massif peridotites. Average and median compositions agree for most of the major elements, with the data approximating a normal distribution (McDonough, 1990). However, the distribution of data for incompatible trace elements (those that do not fit readily into crystal lattice sites, including the HPE) are skewed to higher values, and exhibit a log–normal distribution (Fig. 4). Because there are very few data contents for Th and U of peridotites (these elements are difficult to measure accurately at the low abun-

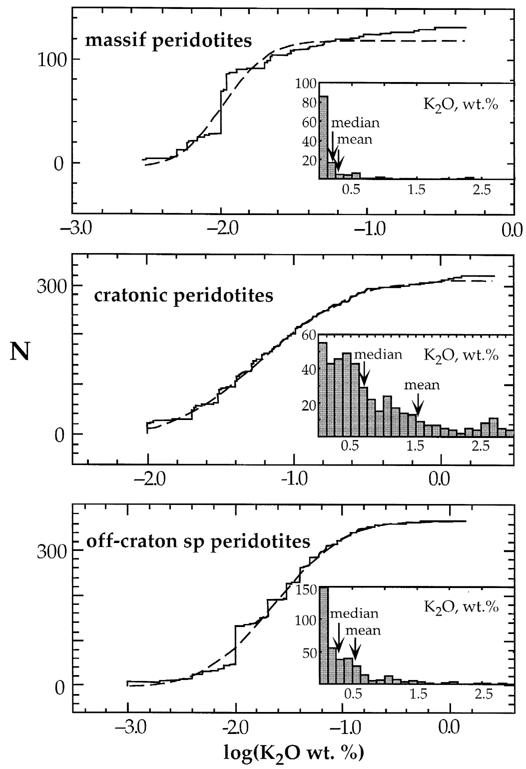

Fig. 4. Cumulative distributions of K_2O analyses for three types of peridotites. The data were fit with an error function $N = a0 + a1\mathrm{erf}((x - a3)/a4)$ where $x = \log(K_2O$ wt%). The fits are shown as dashed lines. Parameters in the fit are: massif: $a0 = 57$, $a1 = 61$, $a2 = -2.0$, $a3 = 0.34$; cratonic: $a0 = 180$, $a1 = 185$, $a2 = -1.6$, $a3 = 0.73$; off-craton: $a0 = 151$, $a1 = 160$, $a2 = -1.2$, $a3 = 0.69$. The massif data could also be fit with two error functions, which are not shown. Insets show histograms of K_2O in wt%.

dances typical of peridotites), we estimate Th and U concentrations from K_2O concentrations using K/U = 10,000 and Th/U = 3.9 (Fig. 1).

If we could be assured that the data compiled from the literature are representative of cratonic mantle, then the average provides the best representation of this population. Indeed, some workers have adopted average K contents of cratonic peridotites to model heat flow in cratonic mantle (e.g., Jordan, 1988). However, Fig. 5 shows that the average garnet peridotite given in Table 5 is too HPE-rich to be representative of cratonic mantle. This figure shows a family of geotherms for 41 mW/m^2 surface heat flow calculated assuming that cratonic roots are composed of average cratonic peridotite (carried as

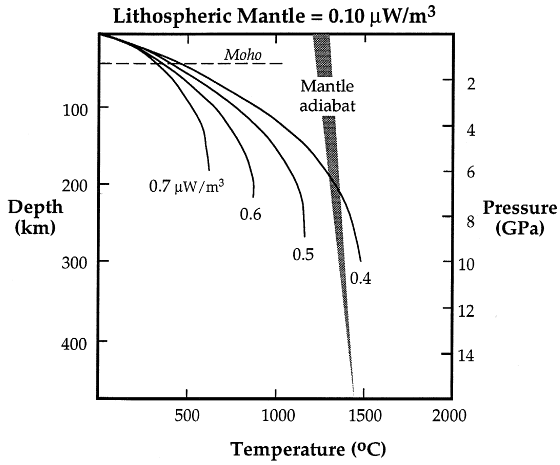

Fig. 5. Conductive geotherms corresponding to surface heat flow of 41 mW/m^2 for a variety of bulk crust compositions (0.4 to 0.7 μW/m^3) and lithospheric mantle composition equal to the average garnet peridotite from kimberlites (0.093 μW/m^3, or 0.15 wt% K_2O, Table 5 column 5). Only the geotherm for the least radiogenic crust composition (0.4 μW/m^3, corresponding to the heat production of average granulites) intersects the mantle adiabat.

xenoliths in kimberlite with 0.148 wt% K_2O, Table 5) and assuming a range of crustal heat production values (0.4, 0.5, 0.6 and 0.7 μW/m^3). The geotherms curve strongly due the high heat production in the lithospheric mantle; only the geotherm corresponding to the lowest crustal heat production of 0.4 μW/m^3 intersects the mantle adiabat. For this geotherm, 40% of the surface heat flow is generated in the continental crust, 36–41% in the lithospheric mantle (depending on absolute thickness, as defined by the intersection of the geotherm and mantle adiabat) and only 19–24% of the heat is derived from the Earth's deep interior. This low crustal heat production corresponds to that of average granulite facies rocks (Pinet and Jaupart, 1987) and is too low to represent bulk Archean continental crust, which is estimated to have a heat production of at least 0.50 to 0.64 μW/m^3 (Table 1). For more reasonable values of crustal heat production (≥ 0.5 μW/m^3), the geotherms never intersect the adiabat —too much heat is generated in the lithospheric mantle.

These observations show that the average HPE content of cratonic peridotite is too high to be representative of Archean mantle roots; cratonic mantle must have lower heat production, but determining its exact composition is not feasible for the following reasons (McDonough, 1990).

(1) Processes such as alteration and host magma infiltration enhance HPE contents of cratonic xenoliths. This is especially important in kimberlite-hosted xenoliths, where late stage phlogopite is commonly seen in fractures and in decompression rims on garnet (e.g., Winterburn et al., 1990).

(2) It is not clear how representative the kimberlite-hosted xenoliths are of mantle through which no kimberlite has erupted. That is, if one could sample cratonic mantle well removed from the site of any kimberlite magmatism, would this mantle show the same amount of metasomatism exhibited by the xenoliths brought up in kimberlite?

(3) K is below analytical detection limits in some samples (particularly the alkali basalt-hosted peridotites), which will therefore not be represented in the database.

(4) There is a tendency for the more exotic varieties of xenoliths, or xenoliths with certain characteristics (e.g., garnet-bearing for thermobarometry) to be collected and studied, thereby biasing the database towards these samples.

Due to these difficulties, the choice of HPE content of cratonic mantle becomes somewhat arbitrary. For our modeling purposes, we chose to use the HPE content of cratonic-like peridotite xenoliths carried in alkali basalts (Table 5) as the best estimate of heat production intrinsic to cratonic mantle roots, as these xenoliths generally do not exhibit the pervasive alteration characteristic of their kimberlite-hosted counterparts. Their mean heat production is a factor of 4 lower than that of kimberlite-hosted cratonic peridotites while their median heat production is slightly higher than that of off-craton spinel peridotite xenoliths (Table 5). Like the other garnet peridotite data, this population is skewed to high values and approximates a log–normal distribution. Because of the relatively small sample population (70 analyses only), we adopt the median value (i.e., 0.03 wt% K_2O, which coincides with the center of the log–normal distribution), for our modeling purposes, assuming that this is better representative of the population than the average. Using this value we calculate the thermal structure of cratonic lithosphere and compare this with the pressure and temperature estimates determined for cratonic garnet peridotites, keeping in mind the qualitative effects of higher heat production on our conclusions.

3.3. Implications for the thermal structure of Archean cratons

Fig. 6 shows a family of geotherms for 41 mW/m^2 surface heat flow calculated using our preferred cratonic peridotite composition (0.03 wt% K_2O, Table 5) and a range of crustal heat production values (0.4, 0.5, 0.6 and 0.7 μW/m^3). Also plotted on this figure are calculated *P–T* points for garnet peridotites from the Archean cratons of South Africa, Tanzania and Siberia. The African data points define a trend at somewhat higher temperatures than the Siberian xenoliths. The only geotherms that come close to matching the xenolith *P–T* points are those for crustal heat production of 0.4 to 0.5 μW/m^3; crust compositions having higher HPE contents (i.e., 0.6 to 0.7 μW/m^3) produce geotherms at considerably lower temperatures. As argued above, it is unlikely that the crustal heat production is as low as 0.4 μW/m^3, but several Archean crustal models have values around 0.5 μW/m^3 (Table 1).

If the xenolith *P–T* points are assumed to represent present-day thermal conditions beneath Archean cratons (i.e., the xenoliths equilibrated to a 41 mW/m^2 geotherm), then our modeling requires low crustal heat production. There are interesting consequences of this. A crustal heat production of 0.5 μW/m^3 corresponds to a crustal contribution of heat flow of 20.5 mW/m^2 — half the observed surface heat flow in Archean cratons. If such a value is correct, it implies that the flux of heat across the Moho is 20.5 mW/m^2 — the same value estimated for many off-craton areas. This, in turn, implies that the difference in surface heat flow between Archean and post-Archean regions is due primarily to changes in bulk crust composition rather than the insulating effects of deep lithospheric roots (cf. Ballard and Pollack, 1987; Lenardic, 1997). In addition, the above observations require that lithospheric thickness does

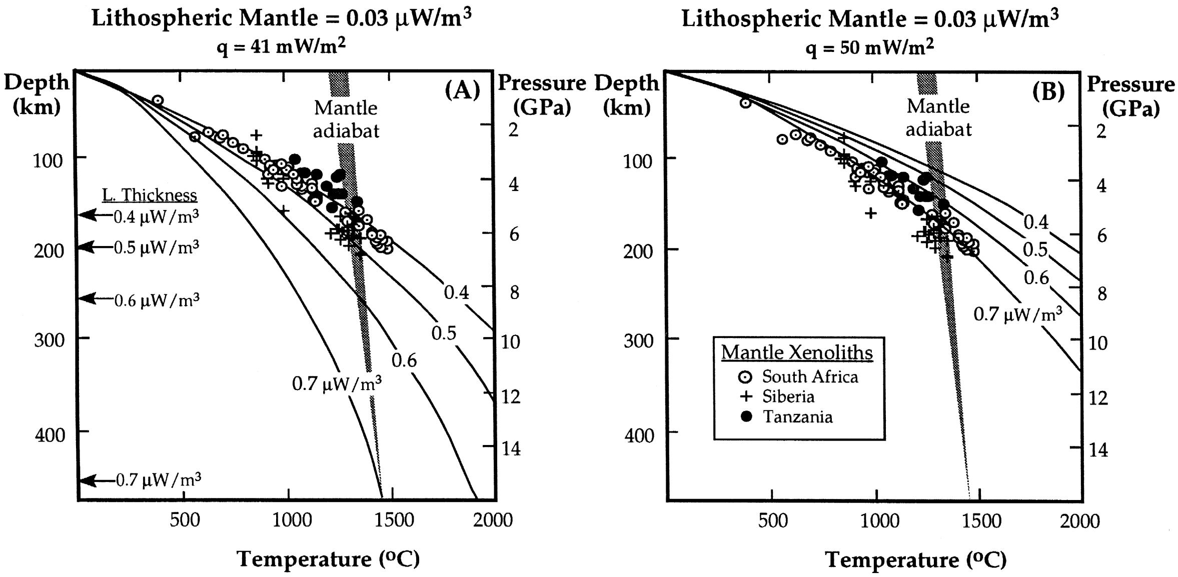

Fig. 6. (A) Conductive geotherms corresponding to surface heat flow of 41 mW/m^2 for a variety of bulk crust compositions (0.4 to 0.7 μW/m^3) and lithospheric mantle composition equal to our best estimate of cratonic peridotite (0.03 μW/m^3, column 10 of Table 5). Xenolith *P–T* points were calculated using the Brey and Köhler (1990) calibrations of the 2 pyroxene thermometer and Al in orthopyroxene barometer. Lithospheric thickness of the different models are marked on the left axis. Cratonic peridotite xenolith *P–T* data points fall between geotherms corresponding to crustal heat production of 0.4 to 0.5 μW/m^3, which corresponds to a lithospheric thickness of less than 200 km. The most radiogenic crust composition at 0.7 μW/m^3 corresponds to 12 mW/m^2 heat flow across the Moho (equivalent to estimates for Moho heat flux in several Archean regions (e.g., Pinet and Jaupart, 1987, Pinet et al., 1991)), but requires a 450 km thick lithosphere, which would extend into the Earth's transition zone. (B) Same as (A) but for 50 mW/m^2 surface heat flow.

not exceed ∼150-200 km depth — the intersection of the adiabat and xenolith data array. (Note that some of the high temperature peridotites, having sheared or porphyroclastic texture and showing evidence of recent melt enrichment (e.g., Smith and Boyd, 1987), have equilibration temperatures above the adiabat and may have been produced by advective heating of the lithosphere).

Our preferred models assume a relatively low lithospheric mantle heat production. If we had used a higher heat production in the lithospheric mantle, the discrepancy between the geotherms and the xenolith *P–T* points is even greater, since the curvature of the geotherms increases with heat production. That is, at higher mantle heat production, even less crustal heat production is required in order for the geotherm to pass through the xenolith *P–T* array. We conclude that, if the xenoliths reflect ambient *P–T* conditions beneath the cratons, then cratonic lithospheric roots are no greater than 150–200 km deep and they play little, if any, role in the observed difference in heat flow between Archean and post-Archean regions. These conclusions appear at odds with seismic data, indicating that anomalously fast (i.e., cold) lithosphere extends to depths of 250–400 km beneath Archean cratons (Jordan, 1975; Su et al., 1995).

Alternatively, if the xenolith *P–T* points reflect either a freezing in of mineral equilibria or paleogeotherms, which may or may not have been conductive at the time of kimberlite eruption (e.g., Harte and Freer, 1982), the lithosphere may be deeper than indicated by the xenoliths. In this scenario, the crust contains a higher concentration of HPE and the ambient geotherms are considerably lower than what the xenoliths record (i.e., they are similar to those for 0.6 and 0.7 $\mu W/m^3$ crustal heat production shown in Fig. 6a). If this is true, then cratonic roots can extend to depths greater than 200 km and the heat flux across the Moho is low (on the order of 12–16 mW/m^2, Table 1). These conditions are consistent with Archean lithospheric roots insulating the continental crust (Ballard and Pollack, 1987; Nyblade and Pollack, 1993).

Fig. 6b shows a family of conductive geotherms calculated for the same conditions in Fig. 6a, but for a surface heat flow of 50 mW/m^2. This illustrates that the xenolith *P–T* data may reflect equilibration to a higher geotherm. Alternatively, they may record a transient thermal pulse to the lithosphere that was present at the time of kimberlite magmatism.

4. A final word on Archean crustal heat production

In Fig. 6a, the curve corresponding to 0.7 $\mu W/m^3$ crustal heat production intersects the adiabat at a depth of ∼450 km. This is deeper than even the deepest seismic models of lithospheric thickness, and would extend the lithosphere into the Earth's transition zone, which begins at ∼410 km. The minimum lithospheric thickness for a crust with this heat production is ∼300 km (Fig. 7), assuming no heat production in the lithospheric mantle. From the relationship between crustal heat production and lithospheric thickness (as defined by the intersection of the geotherms with the adiabat), we can place upper bounds on heat production of Archean continental crust. Fig. 7 shows lithospheric thickness versus

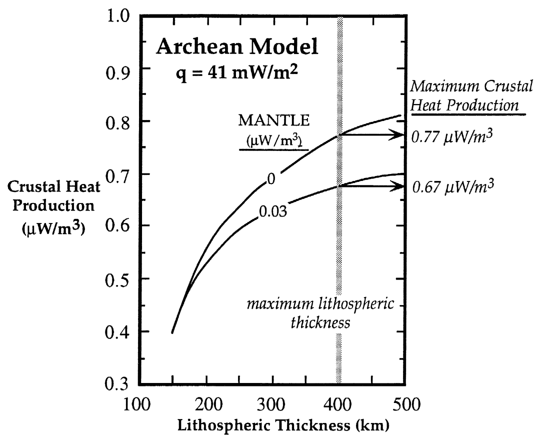

Fig. 7. Lithospheric depth (km) versus crustal heat production for Archean cratons where the surface heat flow is 41 mW/m^2. Two curves are illustrated: zero heat production in the lithospheric mantle and our preferred heat production of 0.03 $\mu W/m^3$. Lithospheric thickness is defined by the intersection of conductive geotherms (calculated according to parameters in Table 4) with the mantle adiabat (see text). Arrows point to maximum crustal heat production for each model. These systematics demonstrate that the uppermost limit to heat production in Archean crust is 0.77 $\mu W/m^3$, and lower values are probably more realistic (i.e., there is heat production in the lithospheric mantle and cratonic lithosphere is likely to be thinner than 400 km).

crustal heat production for a 41 km thick crust and surface heat flow of 41 mW/m^2. If 400 km is considered the upper limit for lithospheric thickness, then the heat production of Archean continental crust must be ≤ 0.77 $\mu W/m^3$. This is an upper limit, as any heat production in the continental lithospheric mantle will give rise to thicker lithosphere (as the geotherms curve over and approach asymptotes to the adiabats). Using our preferred value for cratonic mantle heat production of 0.03 $\mu W/m^3$ gives a maximum crustal heat production of ~ 0.67 $\mu W/m^3$. Thus, we conclude that compositional models for Archean crust having higher heat production (e.g., 0.93 $\mu W/m^3$, Gao et al., 1998) cannot be generally representative of Archean cratons.

5. Conclusions

The average surface heat flow for stable regions of the continents, where heat flow is likely to be mainly conductive, ranges between 47 and 49 mW/m^2 (depending on the non-orogenic heat flow in Phanerozoic crust). Crustal compositional models that produce this much or more surface heat flow are too radiogenic (e.g., the models of Shaw et al., 1986 and Wedepohl, 1995). The remaining crustal models produce less heat flow than this upper limit and are therefore compatible with the heat flow data. Tighter constraints on bulk crust composition from heat flow data require a better understanding of the relative contribution of crust and mantle to surface heat flow.

For a surface heat flow of 41 mW/m^2 (typical of Archean cratons) calculated conductive geotherms are highly variable at lithospheric mantle depths and are most sensitive to the absolute concentration of HPE in the crust and lithospheric mantle. For a range of plausible Archean crust compositions we show that mantle roots beneath Archean cratons cannot have HPE concentrations as high as those observed in average garnet peridotite xenoliths carried in kimberlites, as this produces strongly curved geotherms that do not intersect the mantle adiabat.

Using our best estimate of lithospheric mantle heat production (derived from cratonic-like peridotites carried in non-kimberlitic host magmas), we show that only very unradiogenic bulk crust compositions are consistent with the pressure and temperature points calculated for cratonic garnet peridotite xenoliths. If lithospheric mantle heat production is higher than our estimate, the discrepancy between the xenolith P–T points and conductive geotherms is even greater.

If the xenolith P–T data array does indeed reflect equilibration to a conductive geotherm, then Archean lithosphere is relatively thin (<200 km, based on the intersection of the xenolith P–T array with the mantle adiabat) and the primary reason for the lower surface heat flow in Archean compared to post-Archean crustal regions is differences in crustal radioactivity rather than the insulating effects of thick lithospheric roots. On the other hand, if the xenolith P–T points are regarded as frozen-in mineral equilibria or perturbed geotherms associated with magmatism, then the Archean crust can have higher HPE concentrations, lithospheric thickness can range to greater depths and the difference between Archean and post-Archean surface heat flow is due, at least in part, to the insulating effects of thick lithospheric roots. An uppermost limit to Archean crustal heat production is 0.77 $\mu W/m^3$, which corresponds to a lithospheric thickness of 400 km; 0.67 $\mu W/m^3$ is considered a better estimate. If the lithosphere is thinner than 400 km, the maximum Archean crustal heat production drops accordingly.

Acknowledgements

We thank Joe Boyd for sharing his mineral chemistry data for Kaapvaal and Siberian mantle xenoliths and Carl Agee for discussions on the temperature of transition zone phase changes. We are grateful to Henry Pollack, Dallas Abbott, Scott McLennan and Anton Hales for thoughtful reviews and Andy Nyblade and Geoff Davies for discussions, all of which have led to improvements in the manuscript. This work has been supported by NSF grants EAR 95-06510 to RLR and EAR 95-06517 to WFM.

References

Akaogi, M., Ito, E., Navrotsky, A., 1989. Olivine-modified spinel–spinel transitions in the system Mg_2SiO_4–Fe_2SiO_4: Calorimetric measurements, thermochemical calculation, and geophysical application. J. Geophys. Res. 94, 15671–15685.

Ashwal, L.D., Morgan, P., Kelley, S.A., Percival, J.A., 1987. Heat production in an Archean crustal profile and implications for heat flow and mobilization of heat-producing elements. Earth Planet. Sci. Lett. 85, 439–450.

Ballard, S., Pollack, H.N., 1987. Diversion of heat by Archean cratons: a model for southern Africa. Earth Planet. Sci. Lett. 85, 253–264.

Birch, F., Roy, R.F., Decker, E.R., 1968. Heat flow and thermal history in New England and New York. In: Zen, E., White, W.S., Hadley, J.B., Thompson, J.B. (Eds.), Studies of Appalachian Geology: Northern and Maritime. Interscience, New York, pp. 437–451.

Boyd, F.R., 1989. Compositional distinction between oceanic and cratonic lithosphere. Earth Planet. Sci. Lett. 96, 15–26.

Brey, G.P., Köhler, T., 1990. Geothermobarometry in four-phase lherzolites II. New thermobarometers, and practical assessment of existing thermobarometers. J. Petrol. 31, 1353–1378.

Chapman, D.S., 1986. Thermal gradients in the continental crust. In: Dawson, J.B., Carswell, D.A., Hall, J., Wedepohl, K.H. (Eds.), The Nature of the Lower Continental Crust. Geol. Soc. London Spec. Publ., London, pp. 63–70.

Chesley, J., Rudnick, R.L., 1996. Growth and modification of the Tanzanian lithospheric mantle: preliminary Re–Os results. J. Conf. Abst. 1, 105.

Christensen, N.I., Mooney, W.D., 1995. Seismic velocity structure and composition of the continental crust: a global view. J. Geophys. Res. 100, 9761–9788.

Davies, G.F., Strebeck, J.W., 1982. Old continental geotherms: constraints on heat production and thickness of continental plates. Geophys. J.R. Astron. Soc. 69, 623–634.

Dawson, J.B., Smith, J.V., 1977. The MARID (mica–amphibole–rutile–ilmenite–diopside) suite of xenoliths in kimberlite. Geochim. Cosmochim. Acta 41, 309–323.

Ehrenberg, S.N., 1982. Petrogenesis of garnet lherzolite and megacrystalline nodules from the Thumb, Navajo volcanic field. J. Petrol. 23, 507–547.

Fei, Y., 1995. Thermal expansion. In: Ahrens, T.J. (Ed.), Mineral Physics and Crystallography: A handbook of physical constants. AGU, pp. 29–44.

Fountain, D.M., Salisbury, M.H., Furlong, K.P., 1987. Heat production and thermal conductivity of rocks from the Pikwitonei–Sachigo continental cross section, central Manitoba: implications for the thermal structure of Archean crust. Can. J. Earth Sci. 24, 1583–1594.

Furlong, K.P., Chapman, D.S., 1987. Crustal heterogeneities and the thermal structure of the continental crust. Geophys. Res. Lett. 14, 314–317.

Galer, S.J.G., Goldstein, S.L., O'Nions, R.K., 1989. Limits on chemical and convective isolation in the Earth's interior. Chem. Geol. 75, 257–290.

Gao, S., Luo, T.-C., Zhang, B.-R., Zhang, H.-F., Han, Y.-W., Hu, Y.-K., Zhao, Z.-D., 1998. Chemical composition of the continental crust as revealed by studies in East China. Geochim. Cosmochim. Acta, in press.

Harte, B., Freer, R., 1982. Diffusion data and their bearing on the interpretation of mantle nodules and the evolution of the mantle lithosphere. Terra Cognita 2, 273–275.

Hawkesworth, C.J., Kempton, P.D., Rogers, N.W., Ellam, R.M., van Calsteren, P.W., 1990. Continental mantle lithosphere, and shallow level enrichment processes in the Earth's mantle. Earth Planet. Sci. Lett. 96, 256–268.

Ito, E., Takahashi, E., 1989. Postspinel transformations in the system Mg_2SiO_4–Fe_2SiO_4 and some geophysical implications. J. Geophys. Res. 94, 637–646.

Jaupart, C., 1983. Horizontal heat transfer due to radioactivity contrasts: causes and consequences of the linear heat flow relation. Geophys. J.R. Astron. Soc. 75, 411–435.

Jordan, T.H., 1975. The continental tectosphere. Rev. Geophys. Space Phys. 13, 1–12.

Jordan, T.H., 1988. Structure and formation of the continental tectosphere. J. Petrol., Lithosphere Special Issue: 11–37. Menzies, M.A., Cox, K. (Eds.), Oceanic and Continental Lithosphere: Similarities and Differences.

Ketcham, R.A., 1996. Distribution of heat-producing elements in the upper and middle crust of southern and west central Arizona: evidence from core complexes. J. Geophys. Res. 101, 13611–13632.

Lachenbruch, A.H., 1968. Preliminary geothermal model of the Sierra Nevada. J. Geophys. Res. 73, 6977–6989.

Lenardic, A., 1997. On the heat flow variation from Archean cratons to Proterozoic mobile belts. J. Geophys. Res. 102, 709–721.

McDonough, W.F., 1990. Constraints on the composition of the continental lithospheric mantle. Earth Planet. Sci. Lett. 101, 1–18.

McDonough, W.F., Frey, F.A., 1989. Rare earth elements in upper mantle rocks. In: Lipin, B.R., McKay, G.A. (Eds.), Geochemistry and Mineralogy of Rare Earth Elements. Mineralogical Society of America, Washington, D.C., pp. 99–145.

McLennan, S.M., Taylor, S.R., 1996. Heat flow and the chemical composition of continental crust. J. Geol. 104, 377–396.

Morgan, P., 1984. The thermal structure and thermal evolution of the continental lithosphere. In: Pollack, H.N., Murthy, V.R. (Ed.), Structure and Evolution of the Continental Lithosphere. Phys. Chem. Earth, pp. 107–193.

Navrotsky, A., 1995. Thermodynamic properties of minerals. In: Ahrens, T.J. (Ed.), Mineral Physics and Crystallography: A handbook of physical constants. AGU, pp. 18–28.

Nicolayson, L.O., Hart, R.J., Gale, N.H., 1981. The Vredefort radioelement profile extended to supracrustal strata at Carletonville, with implications for continental heat flow. J. Geophys. Res. 86, 10653–10661.

Nyblade, A.A., Pollack, H.N., 1993. A global analysis of heat flow from Precambrian terrains: implications for the thermal structure of Archean and Proterozoic lithosphere. J. Geophys. Res. 98, 12207–12218.

Pinet, C., Jaupart, C., 1987. The vertical distribution of radiogenic heat production in the Precambrian crust of Norway and Sweden: geothermal implications. Geophys. Res. Lett. 14, 260–263.

Pinet, C., Jaupart, C., Mareschal, J.-C., Gariepy, C., Bienfait, G., Lapointe, R., 1991. Heat flow and structure of the lithosphere in the Eastern Canadian shield. J. Geophys. Res. 96, 19941–19963.

Rhodes, J.M., Dawson, J.B., 1975. Major and trace element chemistry of peridotite inclusion from the Lashaine volcano, Tanzania. In: Ahrens, L.H., Dawson, J.B., Duncan, A.R., Erlank, A.J. (Eds.), Physics and Chemistry of the Earth. Pergamon Press, New York, pp. 545–557.

Roy, R.F., Blackwell, D.D., Birch, F., 1968. Heat generation of plutonic rocks and continental heat flow provinces. Earth Planet. Sci. Lett. 5, 1–12.

Rudnick, R.L., Fountain, D.M., 1995. Nature and composition of the continental crust: a lower crustal perspective. Rev. Geophys. 33, 267–309.

Rudnick, R.L., McDonough, W.F., Orpin, A., 1994. Northern Tanzanian peridotite xenoliths: a comparison with Kaapvaal peridotites and inferences on metasomatic interactions. In: Meyer, H.O.A., Leonardos, O. (Eds.), Kimberlites, Related Rocks and Mantle Xenoliths, vol. 1 (Proceedings Fifth Int. Kimb. Conf.). C.P.R.M., Brasilia, pp. 336–353.

Schatz, J.F., Simmons, G., 1972. Thermal conductivity of earth materials at high temperatures. J. Geophys. Res. 77, 6966–6983.

Schulze, D.J., 1995. Low-Ca garnet harzburgites from Kimberley, South Africa: abundance and bearing on the structure and evolution of the lithosphere. J. Geophys. Res. 100, 12513–12526.

Sclater, J.G., Jaupart, C.J., Galson, D., 1980. The heat flow through oceanic and continental crust and the heat loss of the earth. Rev. Geophys. Space Phys. 18, 269–311.

Shaw, D.M., Cramer, J.J., Higgins, M.D., Truscott, M.G., 1986. Composition of the Canadian Precambrian shield and the continental crust of the earth. In: Dawson, J.B., Carswell, D.A., Hall, J., Wedepohl, K.H. (Eds.), The Nature of the Lower Continental Crust. Geol. Soc. London, London, pp. 257–282.

Smith, D., Boyd, F.R., 1987. Compositional heterogeneities in a high-temperature lherzolite nodule and implications for mantle processes. In: Nixon, P.H. (Ed.), Mantle Xenoliths. Wiley, Chichester, pp. 551–561.

Sobolev, N.V., 1977. Deep-seated inclusions in kimberlites and the problem of the composition of the upper mantle. American Geophysical Union, Washington, D.C., 279 pp.

Su, W.-J., Woodward, R.L., Dziewonski, A.M., 1995. Degree-12 model of shear velocity heterogeneity in the mantle. J. Geophys. Res. 99, 6945–6980.

Taylor, S.R., McLennan, S.M., 1981. The composition and evolution of the continental crust: rare earth element evidence from sedimentary rocks. Phil. Trans. R. Soc. Lond. A 301, 381–399.

Taylor, S.R., McLennan, S.M., 1985. The Continental Crust: its Composition and Evolution. Blackwell, Oxford, 312 pp.

Vitorello, I., Pollack, H.N., 1980. On the variation of continental heat flow with age and the thermal evolution of the continents. J. Geophys. Res. 85, 983–995.

Weaver, B.L., Tarney, J., 1984. Empirical approach to estimating the composition of the continental crust. Nature 310, 575–577.

Wedepohl, H., 1995. The composition of the continental crust. Geochim. Cosmochim. Acta 59, 1217–1239.

Winterburn et al., 1990. Not in reference list. Please supply reference.